Sub-6-GHz Uplink Massive MIMO System Using Holographic Beamforming Metasurfaces: A Conceptual Development

Insang Yoo, *Member, IEEE*, and David R. Smith, *Senior Member, IEEE*

***Abstract*—We propose an uplink massive MIMO system using an array of holographic metasurfaces as a sector antenna operating at 3.5 GHz. The antenna consists of a set of rectangular waveguide-fed metasurfaces combined along the elevation direction into a planar aperture, each with subwavelength-sized metamaterial elements as radiators. The metamaterial radiators are designed such that the waveguide-fed metasurface implements a holographic solution for the guided (or reference) mode, generating a directional beam towards a prescribed direction, thereby forming a multibeam antenna system. We demonstrate that a narrowband uplink massive MIMO system using the metasurfaces can achieve the sum capacity close to that offered by the Rayleigh channel. We show that metasurfaces supporting multiple beams can achieve high spatial resolution in the azimuth directions in sub-6 GHz channels, and thereby form uncorrelated MIMO channels between the base station and users. Also, the proposed metasurface antenna is structurally simple, low-cost, and efficient, and thus is suitable to alleviate RF hardware issues common to massive MIMO systems equipped with a large antenna system.**

***Index Terms*—MIMO systems, multiuser channels, leaky wave antenna, aperture antennas.**

I. Introduction

RECENTLY, multiple-input, multiple-output (MIMO) systems with a large number of base station antennas, referred to as massive MIMO systems, have gained considerable interest due to their capabilities to meet growing demands for high data rates [1], [2]. In massive MIMO systems, the base stations are equipped with many antennas to exploit uncorrelated and even asymptotically orthogonal subchannels that can be provided by the large antenna system [3]. Due to a significant improvement in the spectral efficiency predicted by theoretical studies and prototypes [1], [2], [4], massive MIMO systems are considered key ingredients of current and future communication systems.

The large number of radiating elements in massive MIMO systems, however, poses challenges such as the increased cost, design complexity, and high power consumption associated with array antenna systems and the large number of RF chains (i.e., one for each radiator) [3]. For most sub-6 GHz bands, a full digital beamformer (DBF) is an attractive solution for most MIMO systems as it provides the greatest flexibility in adapting multiple beams to the propagation channels [3]. However, sub-6 GHz massive MIMO systems with a large antenna system (e.g., on the order of hundreds) and low power consumption may require alternative choices for scalable and sustainable antenna and RF systems.

Recently, there has been increasing interest in holographic metasurfaces to address the challenges posed by the increased RF complexity of massive MIMO systems [3]. Among available holographic metasurfaces, we find that waveguide-fed metasurface antennas reported in [5] represent a suitable radiative platform with a simple, low-cost, and low profile configuration that can bring many opportunities to massive MIMO systems. Waveguide-fed metasurface antennas consist of a waveguide that excites metamaterial radiators embedded in its upper conducting layer. In the devices, the metamaterial radiators are excited by the guided modes (i.e., feed wave) and their geometric (or electrical) configurations can be tuned to realize holographic beamforming capabilities without requiring costly and power-hungry RF components [5], [6], which is appealing for massive MIMO systems.

For massive MIMO systems operating in sub-6 GHz bands, the spatial properties of the propagation channels can be exploited to further reduce the RF system complexity. In particular, it is observed in sub-6 GHz band MIMO channels that the angular spread in elevation is generally small compared to that in the azimuth directions [7], [8]; therefore, it is natural to consider a holographic waveguide-fed metasurface antenna with high spatial resolution in the azimuth directions. To implement such a metasurface antenna system, we consider an array of rectangular waveguide-fed metasurfaces patterned so as to generate multiple beams with a greater resolution in the azimuth direction.

In this letter, we present an uplink massive MIMO system using a set of metasurface antennas to form a base station antenna operating at 3.5 GHz. To demonstrate the operation of the system, we design holographic beamforming metasurface antennas, each consisting of a rectangular waveguide and radiating metamaterial elements, and verify their performance using the coupled dipole method. We then demonstrate that the proposed massive MIMO system using the metasurface aperture generating multiple beams can achieve a sum capacity close to that offered by the Raylegh channel.

II. Design of Holographic Metasurface Antennas

We consider a rectangular waveguide-fed metasurface antenna with a set of metamaterial elements that implement a holographic beamforming solution for the guided modes [5],

Manuscript received 12 December 2022; accepted 15 January 2023. Date of publication 17 January 2023; date of current version 11 April 2023. This work was supported by the National Science Foundation (NSF) under Grant 2030068. The associate editor coordinating the review of this article and approving it for publication was L. Zhang. *(Corresponding author: Insang Yoo.)*

The authors are with the Center for Metamaterials and Integrated Plasmonics and the Department of Electrical and Computer Engineering, Duke University, Durham, NC 27708 USA (e-mail: insangyoo1@gmail.com).

Digital Object Identifier 10.1109/LWC.2023.3237761

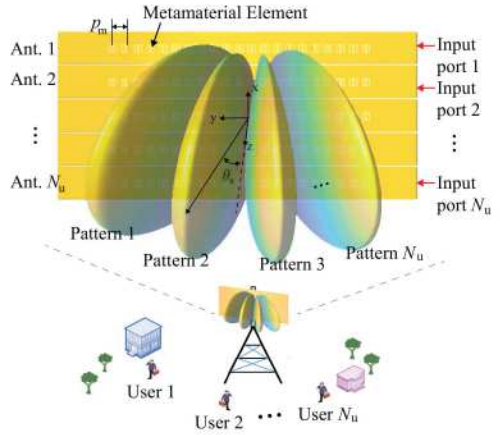

Fig. 1. Schematic of an array of rectangular waveguide-fed metasurface antenna for uplink massive MIMO system. The antenna consists of N_{bs} metasurfaces with metamaterial elements as radiators, and uth metasurface generates a beam toward prescribed direction $\theta = \theta_u$.

as illustrated in Fig. 1. Each metasurface antenna consists of a rectangular waveguide, with resonant metamaterial radiators etched into the upper conductor. Since the elements are electrically small, each element forms a subwavelength aperture that can be modeled as the polarizable magnetic dipole excited by the guided modes [9]. If the element spacing is also subwavelength, they represent a step-wise approximation to a continuous, linear distribution of current density over a conducting plane. Holographic solutions are then easily identified and implemented as the current density that results from the interference of the incident waveguide mode and the desired radiation pattern back-propagated to the aperture [5].

Following the holographic solution in [5], the required polarizabilities for beamforming are obtained such that the phase advance in the feed waveguide is compensated, and the radiated field constructively interferes at a desired direction. For example, for the metasurface antenna shown in Fig. 1, the desired polarizability of ith element located at y_i can be expressed as

$$\alpha_{x,i}^{m,req} = e^{j\beta y_i} e^{jk_0 y_i \cos\theta_0}, \tag{1}$$

where β and k_0 represent the propagation constant and free space wavenumber, respectively. θ_0 is the desired beam direction. However, the available set of polarizabilities supported by resonant metamaterial elements is limited by the Lorentzian resonance [5], [9], given by

$$\alpha_{xx}^{mm}(\omega) = \frac{F_m \omega^2}{\omega_0^2 - \omega^2 + j\omega\gamma_m}, \tag{2}$$

with ω and ω_0 being, respectively, the angular frequency and the angular resonant frequency. F_m and $\gamma_m = \omega_0/2Q_m$ represent a coupling factor, damping factor, respectively, and Q_m is the quality factor of the metamaterial element.

Given the dipolar treatment of individual element, we design metasurface antennas using the coupled dipole method (CDM), an effective analysis and design tool for metasurface antennas [9], [10]. At this point, it should be emphasized that our goal is a conceptual development of an uplink massive MIMO system with holographic beamforming metasurfaces by providing comprehensive analyses of the system using the CDM. Therefore, we use a generic model of metasurfaces that are simulated using the CDM and metamaterial elements characterized by (2), where the holographic design approach is employed as an antenna radiation pattern synthesis technique. The full-wave or experimental verification of the holographic design method can be found in [5], [6], [11].

We consider here an array of N_{bs} rectangular waveguide-fed metasurfaces stacked along the $\hat{x}$ direction, as shown in Fig. 1. Each metasurface has N_m metamaterial elements, each characterized by the Lorentzian parameters $F_m = 3.0 \times 10^{-9}$ m^3 and $Q_m = 10.0$. The spacing between adjacent elements is $p_m = 30.0$ mm. It should be noted that the spacing (i.e., p_m) should be less than the half wavelength ($\lambda/2 = 42.85$ mm at the operating frequency of 3.5 GHz) to avoid generating grating lobes [12]. Also, to keep the CDM valid, the elements should be placed at a distance where higher-order modes have sufficiently decayed [9], [13]. We empirically find that the element spacing needs to be $\gtrsim \lambda/3$ [13] and have chosen the value of p_m, accordingly. We assume that each element can have its resonant frequency $\omega_0/2\pi$ tuned to lie between 3.2 GHz and 3.8 GHz. Note that we choose practical values for the Lorentzian parameters that have not been optimized for the simulated antenna design. The substrate filling the waveguide is assumed to be 1.52-mm-thick Rogers 4003C ($\epsilon_r = 3.55$, $\tan\delta = 0.0027$). The width of each rectangular waveguide is 30.0 mm. The waveguide parameters enable us to analytically determine the waveguide feed mode.

With the above parameters selected, the CDM allows self-consisting modeling of the metasurface using the following matrix equation, given in [9] as

$$\mathbf{G}_{xx}^{mm}\mathbf{m}_x = \mathbf{H}^{inc}, \tag{3}$$

where $\mathbf{m}_x, \mathbf{H}^{inc} \in \mathbb{C}^{N_m \times 1}$ are the effective magnetic dipole moments representing the metamaterial elements and the incident magnetic fields, respectively. The off-diagonal entries of the matrix $\mathbf{G}_{xx}^{mm} \in \mathbb{C}^{N_m \times N_m}$ are the Green's functions [14], and the diagonal entries are the inverse of the polarizabilities, i.e., $(\alpha_{x,i}^m)^{-1}$. The matrix equation takes into account all dipolar interactions between the elements and the waveguide in a metasurface. Note that we apply the Lorentizan-constrained polarizabilities in (3), which are obtained from minimizing the Euclidean distance between the accessible and required polarizabilities [15]. By solving the matrix equation in (3) for the magnetic dipole moments, we can compute the radiation pattern and S-parameter [10].

The far-field pattern of uth metasurface can be computed as the sum of the radiated fields by each radiator in the metasurface, given in [16] as

$$E_u^{rad} = -\sum_{i=1}^{N_m}\left(m_{x,i}\frac{\omega\mu_0 k_0 e^{-jk_0 r_i}}{4\pi r_i}\sin\phi\right), \tag{4}$$

where $r_i = |\bar{r} - \bar{r}_i|$ is the radial distance between the ith element and the origin. μ_0 represents the free space magnetic permeability. Using (4), the directivity can be obtained from

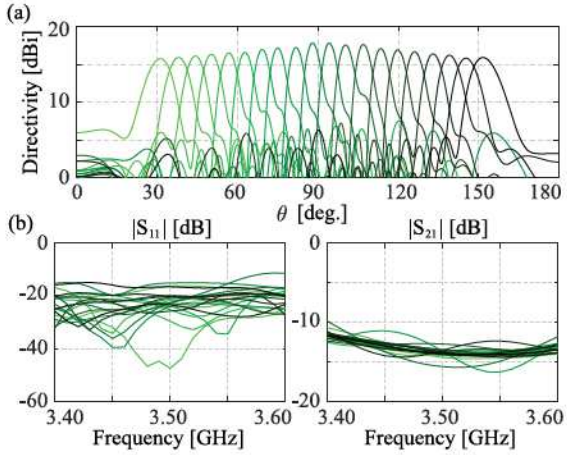

Fig. 2. (a) Directivity patterns of each metasurface antenna at the target frequency of 3.5 GHz. (b) S-parameters of each antenna.

the ratio of the radiated intensity and that of the isotropic radiator [16].

Fig. 2(a) shows the simulated directivity patterns (i.e., radiation patterns on the yz plane) of the designed antenna with $N_{bs} = 20$ metasurfaces, each with $N_m = 30$ metamaterial elements. As the spacing between adjacent metamaterial elements is $p_m = 30$ mm, the overall aperture size is ~ 90 cm $\times$ 60 cm. The operating frequency is chosen to be 3.5 GHz, and each metasurface is designed to generate a beam toward the prescribed directions, ranging from $\theta = 30$ to 150 degrees (with an interval of 6.32°). As shown in Fig. 2(a), the peak directivities of the patterns are maintained to be larger than 15.74 dBi for the designed metasurfaces. Note that the variations in the directivity patterns in Fig. 2(a) are due to changes in the effective aperture area. In other words, as the scan angle moves away from the broadside direction (i.e., $\theta = 90°$), the effective area pointing in the direction of the beam decreases, resulting in a broadened beam with reduced peak directivity. This phenomenon is often referred to as scan loss in antenna engineering [12]. Also, note that each of the radiation patterns shown in Fig. 2(a) is obtained by simulating a metasurface in each row using (3) and computing its pattern using (4). This approach of simulating an array of metasurfaces ignores the mutual interaction of metamaterial elements—through the radiated fields—embedded in waveguides in different rows. However, such interactions of metamaterial elements are often not significant and have minor impacts on antenna's performance [11]. Therefore, we here use the approach to simplify the analysis of the array system rather than introducing an antenna model that accounts for the interactions between all pairs of elements in a metasurface array.

Fig. 2(b) shows the S-parameter of the metasurfaces as a function of frequency, where port "1″ and "2″ of each metasurface indicate the input port (at the right edge of each metasurface) and termination port (at the left edge of each metasurface), respectively. For all of the metasurfaces, it is computed that $S_{11} < -15.62$ dB and $S_{21} < -19.89$ dB at 3.5 GHz. The computed S_{11} indicates that each metasurface has a reasonably good level of impedance match at port 1.

III. Performance Results in Uplink Massive MIMO Systems

We here focus on the analysis of an uplink massive MIMO system where the base station uses the designed metasurface antenna serving one sector in a cell. For the analysis, we assume that each waveguide-fed metasurface in the antenna system is connected to a single RF chain; thus, the base station has N_{bs} RF chains. The maximum number of active users is N_u, and each user terminal is equipped with one dipole antenna. We consider a narrowband, flat-fading propagation channel which yields a received signal, expressed as

$$\mathbf{r} = \sqrt{\rho}\mathbf{H}\mathbf{s} + \mathbf{n}, \tag{5}$$

where $\mathbf{s} \in \mathbb{C}^{N_u \times 1}$ is the transmit signal vector normalized such that $\mathbb{E}[|\mathbf{s}|^2] = 1$, and $\mathbf{r} \in \mathbb{C}^{N_{bs} \times 1}$ is the receive signal vector. Also, $\mathbf{n} \in \mathbb{C}^{N_u \times 1}$ represents a complex Gaussian noise with zero-mean and unit covariance. $\mathbf{H} \in \mathbb{C}^{N_{bs} \times N_u}$ is the channel matrix such that $\mathbb{E}[||\mathbf{H}||_F^2] = N_{bs}N_u$ where $||\cdot||_F^2$ represents the Frobenius norm. ρ is the signal-to-noise power ratio at the receive antenna.

To simulate MIMO propagation channels, we consider a clustered channel model, referred to as the Saleh-Valenzuela (SV) model [17], [18]. The SV model is a physical wireless channel model that statistically describes the angles of arrival (AoA) and departure (AoD) of multipath components [17], [18]. Each entry of the channel matrix $\mathbf{H}$ in this model can be obtained by summing up the contributions of the rays in the clusters, which are multiplied by the channel gain, and transmit and receive antenna gain at the AoA and AoD. More specifically, the entry in the mth row and nth column of the channel matrix $\mathbf{H}$ in (5) can be written as

$$[\mathbf{H}]_{mn} = \sqrt{\frac{1}{N_c N_r}} \sum_{p=1}^{N_c} \sum_{q=1}^{N_r} h_{pq}\, g_n^u\left(\theta_{pq}^u\right) g_m^{bs}\left(\theta_{pq}^{bs}\right), \tag{6}$$

where N_c and N_r represent the number of clusters in the propagation environment and rays in each cluster, respectively. h_{pq} is the complex gain of the qth ray in pth cluster and is assumed to be Rayleigh fading coefficient. $g_n^u(\theta_{pq}^u)$ and $g_m^{bs}(\theta_{pq}^{bs})$ are the antenna gain at the nth user terminal and mth base station, respectively, where θ_{pq}^u and θ_{pq}^{bs} are the transmit and receive angles of the rays. The antenna gain in (6) was computed by using the directivity, where the antenna efficiency was assumed to be unity. Note that θ_{pq}^u and θ_{pq}^{bs} are generated according to a Laplacian distribution with a mean cluster angle θ_{mean}^u, θ_{mean}^{bs} and angular spread σ^u, σ^{bs}, respectively. In constructing the channel matrix $\mathbf{H}$ using (6), we assume that the clusters are independent, and the mean clusters are generated according to the uniform distribution with $\theta_{mean}^u \in [0°, 360°]$ and $\theta_{mean}^{bs} \in [-60°, 60°]$. It should be noted in (6) that we assume that the rays are confined to the yz plane in Fig. 1 (i.e., $\phi = 90°$), as the angle spread in the xz plane is generally small compared to that in the yz plane in sub-6 GHz MIMO channels [7], [8].

To demonstrate the operation of the proposed uplink massive MIMO system, we simulated the system according to (5) and (6), where the radiation patterns of the metasurfaces are incorporated to construct the MIMO channel matrix $\mathbf{H}$. To evaluate

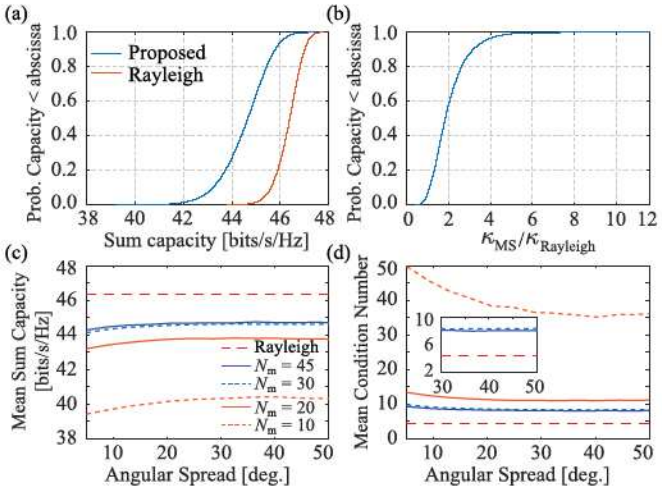

Fig. 3. The cumulative distribution of (a) the sum capacity and, (b) the ratio of the condition numbers of MIMO channel matrix, i.e., $\kappa_{MS}/\kappa_{Rayleigh}$. It is assumed that the angular spread is $\sigma^u = \sigma^{bs} = 20°$. Mean of (c) the sum capacity and, (d) the condition number of MIMO channel matrix. The aperture size of the antenna is varied by changing the number of metamaterial elements N_m, while fixing the number of metasurfaces N_{bs} and the spacing p_m between the elements. The angle spread $\sigma^u = \sigma^{bs}$ is also swept from 5° to 50°.

the performance of the proposed system, we use the condition number κ of the matrix $\mathbf{H}$ and the sum capacity over 10,000 realizations of the channel matrix. Note that $(\cdot)^H$ is the Hermitian operator. In constructing the channel matrix, we assume that the number of clusters and rays are $N_c = 6$ and $N_r = 11$, respectively, which are used to model macro-cells in urban areas [19]. In the simulations, we further assume that the channel state information is available to the base station, and the users do not cooperate with each other. Under these assumptions, the sum capacity can be expressed as [20], [21]

$$C_{sum} = \sum_{u=1}^{N_u} \log_2\left(1 + \frac{\rho}{N_u}\lambda_u\right), \tag{7}$$

where λ_u represents the uth eigenvalue of the matrix $\mathbf{H}^H\mathbf{H}$.

Fig. 3(a) shows the cumulative distribution (CDF) of the sum capacity for the angle spread $\sigma^u = \sigma^{bs} = 20°$ and $\rho = 10$ dB for the antenna with $N_{bs} = 20$ metasurfaces. Each metasurface is assumed to have $N_m = 30$ metamaterial elements—thus, we use the radiation patterns of the antenna shown in Fig. 2(a) in the simulations. It is shown in Fig. 3(a) that the sum capacity offered by the metasurface antenna is close to that by the Rayleigh channel. To evaluate the quality of the subchannels, we compute the ratio of the condition number, i.e., $\kappa_{MS}/\kappa_{Rayleigh}$. κ_{MS} and $\kappa_{Rayleigh}$ represent the condition number of the channel matrix $\mathbf{H}$ in (6) and that of the Rayleigh channel matrix, respectively. Fig. 3(b) shows the CDF of the ratio of the condition number for the angle spread $\sigma^u = \sigma^{bs} = 20°$, illustrating that the condition number of the MIMO channels provided by the proposed system is comparable to Rayleigh channel. It should be noted at this point that the number of beams, beam widths, and beam angles should be determined by examining the system performance metrics, such as the sum rate. For example, having sharp beams can help minimize spatial correlation. However, if beams are too narrow and do not overlap, regions between two adjacent beams may result in very weak signal strength and poor communication links. In this letter, given the antenna size (i.e., the number of metamaterial radiators N_m and their spacing p_m), we have empirically found the set of beam angles that provide a reasonably high sum rate, illustrated in Fig. 3(a).

We also study the effects of the aperture size of the antenna and angular spread of the clusters on the performance of the proposed massive MIMO system. To alter the aperture size of the antenna, we sweep the number of metamaterial elements N_m from 10 to 45, while fixing the number of metasurfaces to be $N_{bs} = 20$ and the spacing between adjacent metamaterial elements to be $p_m = 30$ mm. For each N_m, we simulate the metasurfaces using the CDM in (3) and compute their radiation patterns. We then use the computed radiation patterns in (6) to construct the channel matrix for each angle spread, varied from 5° to 50°. For the analysis, we generated 10,000 channels for each value of angular spread. In the simulations, we fixed $\rho = 10$ dB.

In the analyses, we used the mean of the sum capacity over the realized MIMO channels as a metric to evaluate the performance of the proposed system. Fig. 3(c) shows the mean of the sum capacity for the swept angle spread (i.e., $\sigma^u = \sigma^{bs}$) and number of elements N_m. As depicted in Fig. 3(c), the mean capacity increases as the number of the metamaterial elements increases, which can be attributed to the increased spatial resolution due to the increased aperture size. Note that the mean of the sum capacity is saturated for $N_m \geq 30$ and approaches 44.75 bits/s/Hz, which is close to that offered by Rayleigh channel, 46.34 bits/s/Hz. Also, for fixed N_m, the mean of the sum capacity is improved with increasing angular spread, as a result of the fixed spatial resolution.

Such observations in the mean of sum capacity in Fig. 3(c) can be demonstrated using the mean of the condition number of the realized channel matricies, as depicted in Fig. 3(b). As shown in Fig. 3(d), the increase in the aperture size (by increasing N_m) results in increased spatial resolution, leading to a reduced spatial correlation between subchannels. More specifically, the mean condition number of the proposed system reaches its minimum of 8.15 for $\sigma^u = \sigma^{bs} \geq 30°$. Note that the mean condition number of the Rayleigh channel is 4.53. Also, it can be observed in Fig. 3(d) that the increase in the angle spread leads to the reduced correlation between subchannels for a fixed number of elements N_m, which is the result of the fixed spatial resolution by the metasurfaces.

In this letter, we have assumed simple communication environments and have not considered the angle spread in the elevation direction to present a conceptual development of the proposed system. However, the angle spread in the elevation should be considered in practical communication systems, and thus, improved spatial resolution along the elevation angle is needed to reduce spatial correlation and mitigate interference. The improved elevation spatial resolution can be achieved by stacking more metasurfaces and using each subset backed by a single RF chain.

Also, it is worth noting that individual metamaterial radiators in each metasurface can be loaded with low-power-driven

tuning elements—such as diodes [6], [22], or liquid crystals—to realize dynamically reconfigurable radiation patterns. The tunable metamaterial radiators will thus allow optimization of the performance of the proposed system by allowing multi-user beamforming capabilities. For instance, each dynamic metasurface can generate and steer a beam toward each user, thereby establishing separate wireless channels for the users. Also, the reconfigurable patterns of the dynamic metasurfaces can be used for interference mitigation by altering the patterns to locate a null at the direction of interference signal, which is a useful capability for small cell networks (e.g., femto cells). The analysis and optimization of such systems remain essential steps for future work.

IV. Conclusion

In this letter, we have proposed an uplink massive MIMO system using an array of rectangular waveguide-fed metasurfaces operating at 3.5 GHz generating multiple beams. In the proposed system, the spatial properties of sub-6 GHz band MIMO channels, as well as the structural advantages of the metasurface antennas, are exploited to further reduce the RF complexity of the MIMO system. We also demonstrated the design of the metasurfaces using the holographic beamforming technique and the coupled dipole method. Using the designed antenna, we showed that a MIMO system using the metasurface antennas can offer a sum capacity approaching that of the Rayleigh channel. As the metasurface antennas are efficient, low-cost, and low-profile, the proposed massive MIMO system using the metasurfaces can find applications in various sub-6 GHz wireless networks requiring a large antenna system. The advantageous traits of the proposed systems can also find its utility in high frequency (e.g., mm-wave bands) or small cell networks under strict energy and cost constraints.

References

[1] T. L. Marzetta, "Noncooperative cellular wireless with unlimited numbers of base station antennas," *IEEE Trans. Wireless Commun.*, vol. 9, no. 11, pp. 3590–3600, Nov. 2010.

[2] E. G. Larsson, O. Edfors, F. Tufvesson, and T. L. Marzetta, "Massive MIMO for next generation wireless systems," *IEEE Commun. Mag.*, vol. 52, no. 2, pp. 186–195, Feb. 2014.

[3] E. Björnson, L. Sanguinetti, H. Wymeersch, J. Hoydis, and T. L. Marzetta, "Massive MIMO is a reality—What is next? Five promising research directions for antenna arrays," *Digit. Signal Process.*, vol. 94, pp. 3–20, Nov. 2019.

[4] J. Vieira et al., "A flexible 100-antenna testbed for massive MIMO," in *Proc. IEEE Globecom Workshops*, 2014, pp. 287–293.

[5] D. R. Smith, O. Yurduseven, L. P. Mancera, P. Bowen, and N. B. Kundtz, "Analysis of a waveguide-fed metasurface antenna," *Phys. Rev. Appl.*, vol. 8, no. 5, 2017, Art. no. 54048.

[6] M. Boyarsky, T. Sleasman, M. F. Imani, J. N. Gollub, and D. R. Smith, "Electronically steered metasurface antenna," *Sci. Rep.*, vol. 11, no. 1, pp. 1–10, 2021.

[7] "Spatial channel model for multiple input multiple output (MIMO) simulations (release 6), vol. 6.1.0," 3GPP, Sophia Antipolis, France, Rep. TR 25.996, 2003. [Online]. Available: http://www.3gpp.org

[8] Q. H. Spencer, B. D. Jeffs, M. A. Jensen, and A. L. Swindlehurst, "Modeling the statistical time and angle of arrival characteristics of an indoor multipath channel," *IEEE J. Sel. Areas Commun.*, vol. 18, no. 3, pp. 347–360, Mar. 2000.

[9] L. Pulido-Mancera, P. T. Bowen, M. F. Imani, N. Kundtz, and D. Smith, "Polarizability extraction of complementary metamaterial elements in waveguides for aperture modeling," *Phys. Rev. B, Condens. Matter*, vol. 96, no. 23, 2017, Art. no. 235402.

[10] L. Pulido-Mancera, M. F. Imani, and D. R. Smith, "Discrete dipole approximation for simulation of unusually tapered leaky wave antennas," in *IEEE MTT-S Int. Microw. Symp. Dig.*, 2017, pp. 409–412.

[11] L. Pulido-Mancera, M. F. Imani, P. T. Bowen, N. Kundtz, and D. R. Smith, "Analytical modeling of a two-dimensional waveguide-fed metasurface," 2018, *arXiv:1807.11592*.

[12] R. J. Mailloux, *Phased Array Antenna Handbook*. Norwood, MA, USA: Artech House, 2005.

[13] I. Yoo and D. R. Smith, "Design of conformal array of rectangular waveguide-fed metasurfaces," *IEEE Trans. Antennas Propag.*, vol. 70, no. 7, pp. 6060–6065, Jul. 2022.

[14] R. E. Collin, *Field Theory of Guided Waves*. New York, NY, USA: McGraw-Hill, 1960.

[15] P. T. Bowen, M. Boyarsky, L. M. Pulido-Mancera, D. R. Smith, O. Yurduseven, and M. Sazegar, "Optimizing polarizability distributions for metasurface apertures with Lorentzian-constrained radiators," 2022, *arXiv:2205.02747*.

[16] C. A. Balanis, *Antenna Theory: Analysis and Design*. New York, NY, USA: Wiley, 2005.

[17] A. A. M. Saleh and R. Valenzuela, "A statistical model for indoor multipath propagation," *IEEE J. Sel. Areas Commun.*, vol. 5, no. 2, pp. 128–137, Feb. 1987.

[18] J. W. Wallace and M. A. Jensen, "Modeling the indoor MIMO wireless channel," *IEEE Trans. Antennas Propag.*, vol. 50, no. 5, pp. 591–599, May 2002.

[19] A. F. Molisch, "A generic model for MIMO wireless propagation channels in Macro-and microcells," *IEEE Trans. Signal Process.*, vol. 52, no. 1, pp. 61–71, Jan. 2004.

[20] J. R. Pêrez, R. P. Torres, M. Domingo, L. Valle, and J. Basterrechea, "Analysis of massive MIMO performance in an indoor picocell with high number of users," *IEEE Access*, vol. 8, pp. 107025–107034, 2020.

[21] R. W. Heath and A. Lozano, *Foundations of MIMO Communication*. Cambridge, U.K.: Cambridge Univ. Press, 2018.

[22] T. Sleasman et al., "Waveguide-fed tunable metamaterial element for dynamic apertures," *IEEE Antennas Wireless Propag. Lett.*, vol. 15, pp. 606–609, 2016.